Electronic Supplementary Material (ESI) for Physical Chemistry Chemical Physics.

Supplementary information

Varying oxygen coverage on Cu_{55} and its effect on CO oxidation

Li Ma[1] and Jaakko Akola[1,2,a)]

[1]Computational Physics Laboratory, Tampere University, P.O. Box 692, FI-33014 Tampere, Finland

[2]Department of Physics, Norwegian University of Science and Technology, NO-7491 Trondheim, Norway

[a)] Author to whom correspondence should be addressed. E-mail: jaakko.akola@ntnu.no

Stepwise adsorption of O_2 molecules

There are twenty equivalent triangular fcc(111)-like facets in the icosahedral Cu_{55} cluster (Figure S1). We began with the optimal $Cu_{55}O_2$ configuration, which was obtained through considering the symmetrically inequivalent atop, bridge, and face binding sites, including different molecular orientations. The most stable adsorption is the bi-dentate mode as the first geometry in Fig. S2, which is the same with the structure in Ref. 1. Repeating this procedure with the next O_2 molecule on all vacant sites in the rest triangular faces step by step, we obtained the most stable configurations of $Cu_{55}O_4$, $Cu_{55}O_6$ and so on. In total, more than 100 initial structures were considered to obtain the most favourable adsorption site for each O_2. The type of adsorption is evident based on the O-O distance: In molecular adsorption, the O-O separation is between 1.45-1.65 Å, while in dissociative adsorption, the O atoms are separated by at least 2.90 Å.

In some cases, the relaxation process led to a spontaneous O_2 dissociation to atomic oxygen. The lowest-energy configurations of $Cu_{55}O_{2N}$ complexes with the increasing number of dissociated O_2 molecules are given in Fig. S2. The full set of geometries for the stepwise adsorption of O_2 molecules for N = 1-20 are shown in Fig. S3. The complexes of this Approach 1 (see the main text) are labeled $(O_2)_M(O)_{2D}$ to indicate the number of O_2 units added to Cu_{55} either molecularly (M) or dissociatively (D), where N = M + D. For N = 1-4, the most stable conformations are molecular adsorption with O_2 located on the neighboring triangular faces. However, the relaxation led to dissociation of O_2 with the increasing of O_2 molecules. The dissociative adsorption appears at N = 5 with one O_2 molecule dissociated to oxygen atoms $(O_2)_4(O)_2$. As the O_2 units increase further, the dissociative adsorption prevails. The number of O_2 dissociation increases from two to seven at N = 7, 11, 12, 14, 15 and 16. For N = 17-20, the additional O_2 keeps molecular adsorption in the complex. There are common characteristics for the O_2 adsorption geometries. Dissociated O atoms preferentially occupy three-fold hollow sites and two-fold edge sites. By contrast, molecularly adsorbed O_2 units attach to bi-dentate sites and bridge sites. In the molecular adsorption, the bond lengths of O_2 significantly expand

from the gas-phase value of 1.23 Å to 1.45-1.65 Å. The lengths and bond orders of O_2 molecules indicate that the O-O bonds are activated in the adsorption process, not to mention the automatic dissociation to oxygen atoms in some cases (Fig. S2). A DFT-MD simulation was performed for ten O_2 molecules adsorbed on Cu_{55} at room temperature (300 K). The obtained structure is in Fig. S4. Compared with the adsorption complex of $Cu_{55}(O_2)_8(O)_4$ at 0 K, the number of dissociated O_2 molecules increases rapidly from two to nine at 300 K [$Cu_{55}(O_2)(O)_{18}$] leaving only one O_2 intact. This confirms the spontaneous dissociation of O_2.

The energies of $E_a(N)$ and $\langle E_a(N) \rangle$ versus the number of O_2 added on Cu_{55} cluster are plotted for Approach 1 in Fig. S5. The corresponding energy values and the electronic and geometric properties are listed in Table S1. The trends in $E_a(N)$ for the $Cu_{55}(O_2)_M(O)_{2D}$ complexes (Fig. S5) clearly show that dissociative adsorption is preferred: $E_a(N)$ is higher than 2.0 eV for the dissociative cases, while it keeps around 1.3 eV until $Cu_{55}(O_2)_9(O)_8$ for molecular adsorption. $E_a(N)$ decreases to less than 1.0 eV for $N \geq 17$. It should be noted that the adsorption energy of N = 20 is -0.13 eV, which indicates that a saturated structure is achieved at N = 19. The second column of Fig. S5 shows the average adsorption energy $\langle E_a(N) \rangle$ of the total O_2. The $\langle E_a(N) \rangle$ generally increases with the number of O_2 until N=16. Thus, the adsorption complexes can continue to gain energy during the adding process. The appearance of local peaks are consistent for $E_a(N)$ and $\langle E_a(N) \rangle$, indicating spontaneous O_2 dissociation at these points.

As expected, oxygen adsorption leads to electron transfer from the Cu_{55} to the oxygen, leaving the Cu_{55} core with a net positive charge (Table S1). Moreover, the charge transfer increases with the number of oxygen except for N = 20, which is correlated with the interaction strength between Cu_{55} and O_2. The averaged effective charge is ~1.0 *e* on every dissociated O which is nearly two times higher than that of molecularly adsorbed O (Table S1). For Cu_{55}, oxygen adsorption results in a clear increase in the average <Cu-Cu> bond length. In comparison with 2.544 Å in the isolated Cu_{55} cluster,

<Cu-Cu> increases from 2.547 to 2.662 Å as N increases from 1 to 20 (Table S1), which reflects the severe distortion of the Cu_{55} cluster geometry as oxygen adsorption proceeds.

Reference

1. D Tang and J Zhang, *RSC Adv.*, 2013, **3**, 15225-15236.

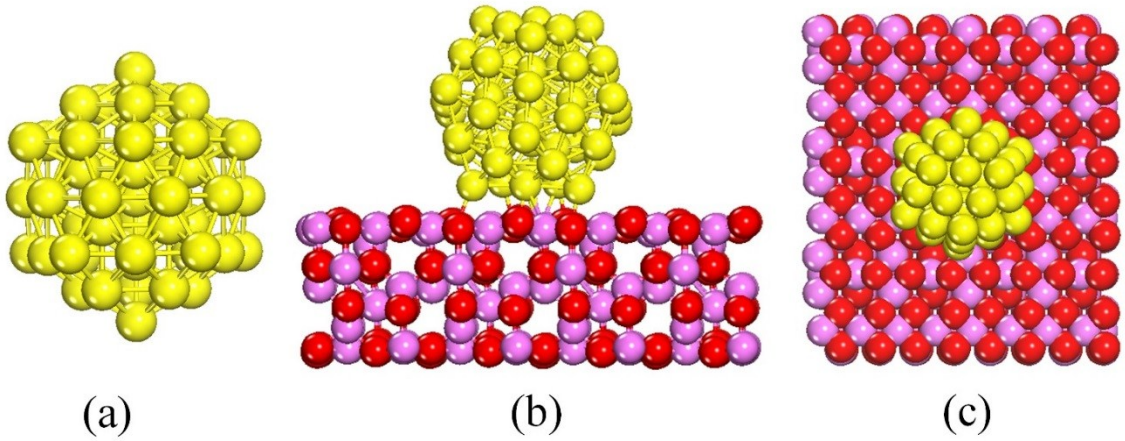

Fig. S1 Optimized geometries of (a) Cu_{55}, (b) side view of Cu_{55}/γ-Al_2O_3(100) and (c) top view of Cu_{55}/γ-Al_2O_3(100). Color key: Cu, yellow; Al, violet; O, red.

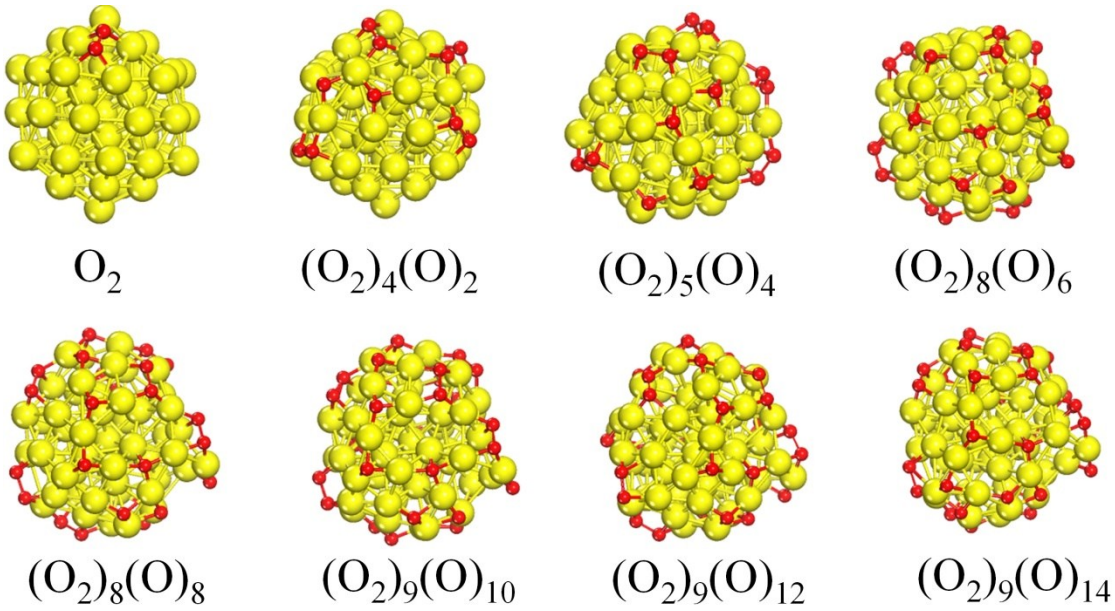

Fig. S2 Geometries of $Cu_{55}O_{2N}$ with the number of dissociated O_2 increasing from zero to seven at N = 1, 5, 7, 11, 12, 14, 15, 16 (Approach 1). The labeling $(O_2)_M(O)_{2D}$ indicates the number of O_2 units molecularly (M) and/or dissociatively (D) adsorbed.

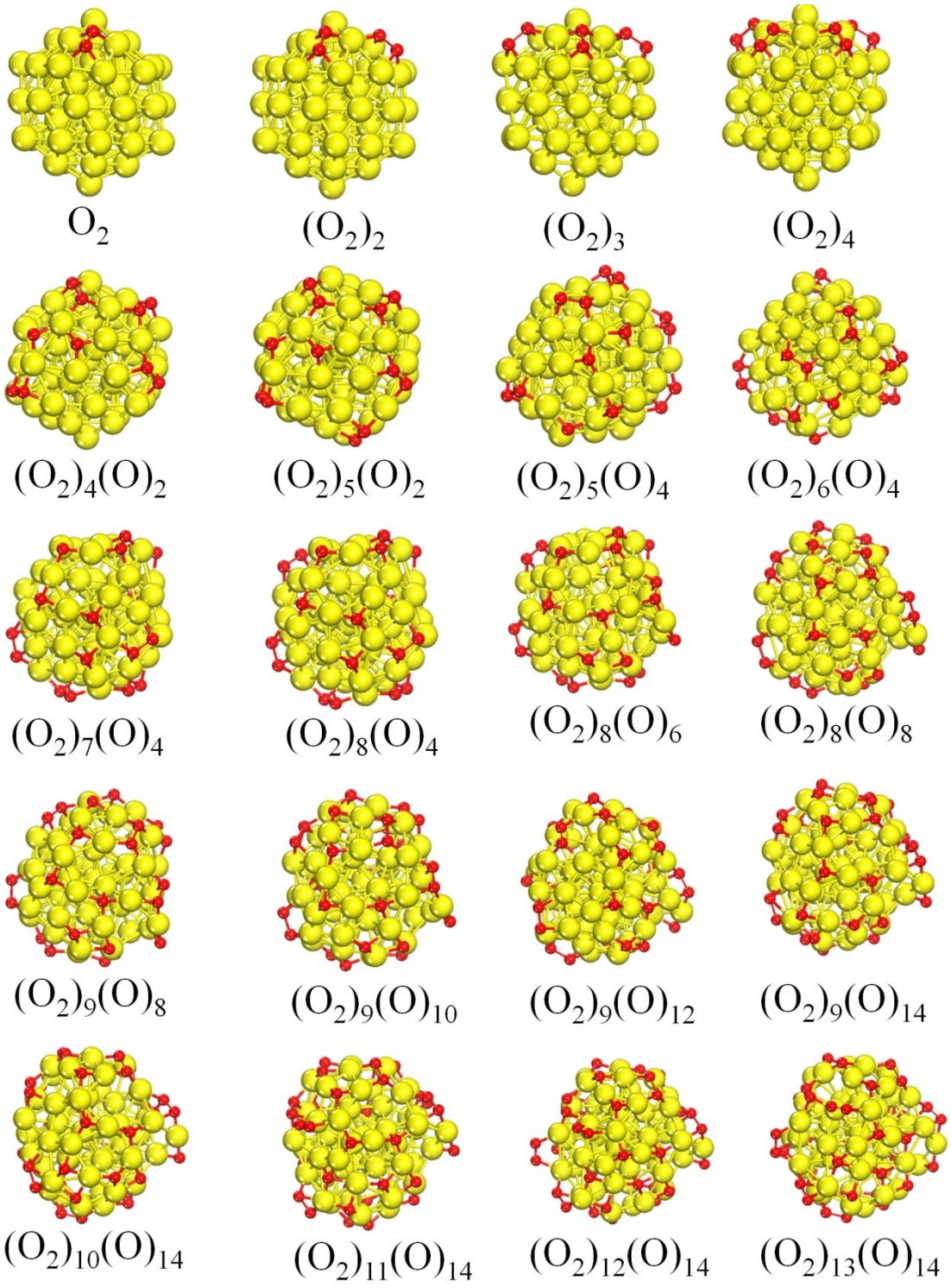

Fig. S3 The full set of geometries for the stepwise adsorption of O_2 molecules (N = 1-20) on Cu_{55} (Approach 1).

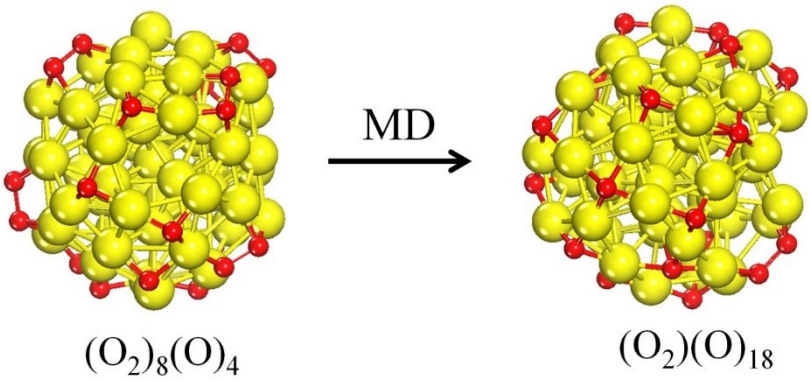

Fig. S4 Geometries of $Cu_{55}O_{2N}$ (N = 10) at 0 K and after 20 ps of MD at 300 K. Most O_2 dissociate already during this short simulation highlighting the instability of molecular oxygen.

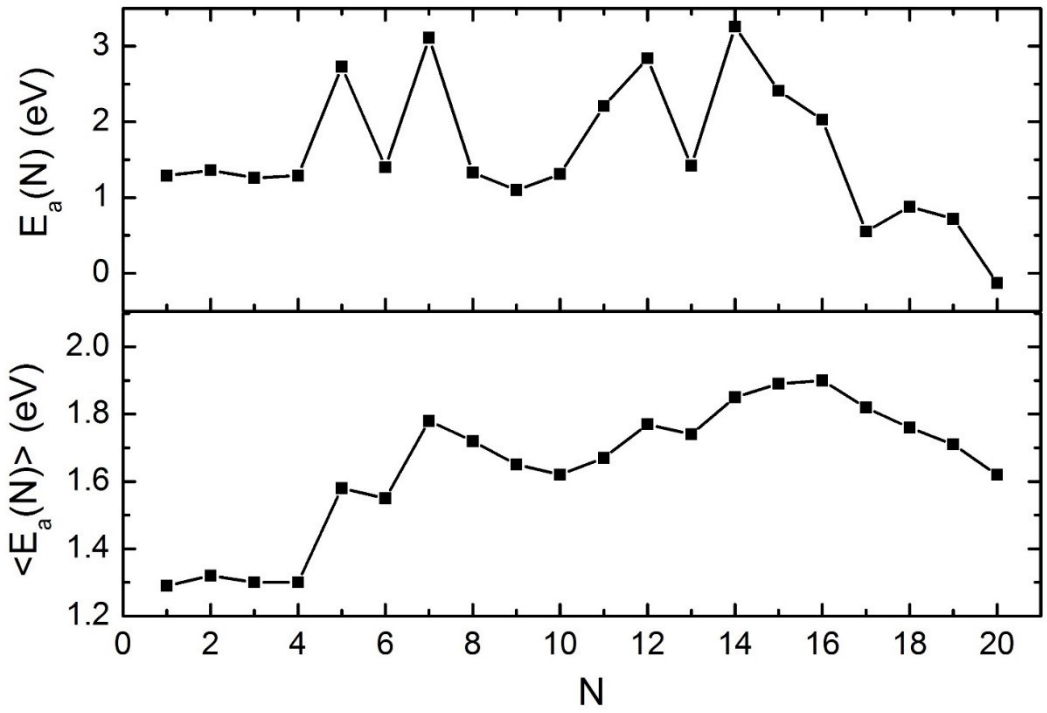

Fig. S5 Adsorption energy $E_a(N)$ of each O_2 and average adsorption energy $\langle E_a(N) \rangle$ of added O_2 molecules versus the number of O_2 added on Cu_{55} cluster (Approach 1). The spontaneous oxygen dissociation is visible as pronouncedly large values in $E_a(N)$. Note that this calculation is performed at 0 K and all O_2 molecules are likely to dissociate under realistic conditions since they have small reaction barriers.

Table S1 Properties of the stepwise O_2 adsorption complexes $Cu_{55}O_{2N}$ (N=1-20, Approach 1).[a]

N ($Cu_{55}O_{2N}$)	$(O_2)_M(O)_{2D}$	$E_a(N)$ (eV)	$< E_a(N) >$ (eV)	Q_{Cu55} (e)	Q_O (e) $(O_2)_M$	$(O)_{2D}$	<Cu-Cu> (Å)
1	O_2	1.29	1.29	1.22	-0.61		2.547
2	$(O_2)_2$	1.36	1.32	2.40	-0.60		2.551
3	$(O_2)_3$	1.26	1.30	3.44	-0.57		2.559
4	$(O_2)_4$	1.29	1.30	4.65	-0.58		2.565
5	$(O_2)_4(O)_2$	2.73	1.58	6.54	-0.56	-1.01	2.565
6	$(O_2)_5(O)_2$	1.40	1.55	7.63	-0.56	-0.97	2.567
7	$(O_2)_5(O)_4$	3.11	1.78	9.60	-0.54	-1.04	2.574
8	$(O_2)_6(O)_4$	1.33	1.72	10.70	-0.58	-0.90	2.583
9	$(O_2)_7(O)_4$	1.10	1.65	12.09	-0.55	-1.09	2.584
10	$(O_2)_8(O)_4$	1.31	1.62	12.73	-0.55	-0.97	2.595
11	$(O_2)_8(O)_6$	2.21	1.67	15.04	-0.54	-1.04	2.597
12	$(O_2)_8(O)_8$	2.84	1.77	16.60	-0.56	-0.94	2.608
13	$(O_2)_9(O)_8$	1.42	1.74	18.29	-0.54	-1.05	2.611
14	$(O_2)_9(O)_{10}$	3.26	1.85	20.10	-0.54	-1.02	2.615
15	$(O_2)_9(O)_{12}$	2.41	1.89	21.14	-0.52	-0.97	2.635
16	$(O_2)_9(O)_{14}$	2.03	1.90	23.56	-0.56	-0.95	2.644
17	$(O_2)_{10}(O)_{14}$	0.55	1.82	24.34	-0.54	-0.95	2.652
18	$(O_2)_{11}(O)_{14}$	0.88	1.76	25.23	-0.52	-0.98	2.652
19	$(O_2)_{12}(O)_{14}$	0.72	1.71	25.73	-0.50	-0.97	2.661
20	$(O_2)_{13}(O)_{14}$	-0.13	1.62	25.41	-0.45	-0.97	2.662

[a]$E_a(N)$ is the adsorption energy of the last molecular or dissociative adsorption on Cu_{55}. $< E_a(N) >$ is the average adsorption energy of the added O_2 molecules. Q_{Cu55} is the total charge on Cu_{55} cluster. Q_O are average charge on every molecular $(O_2)_M$ and dissociative $(O)_{2D}$ adsorption O atom, respectively. <Cu-Cu> is the average Cu-Cu bond length in the cluster.

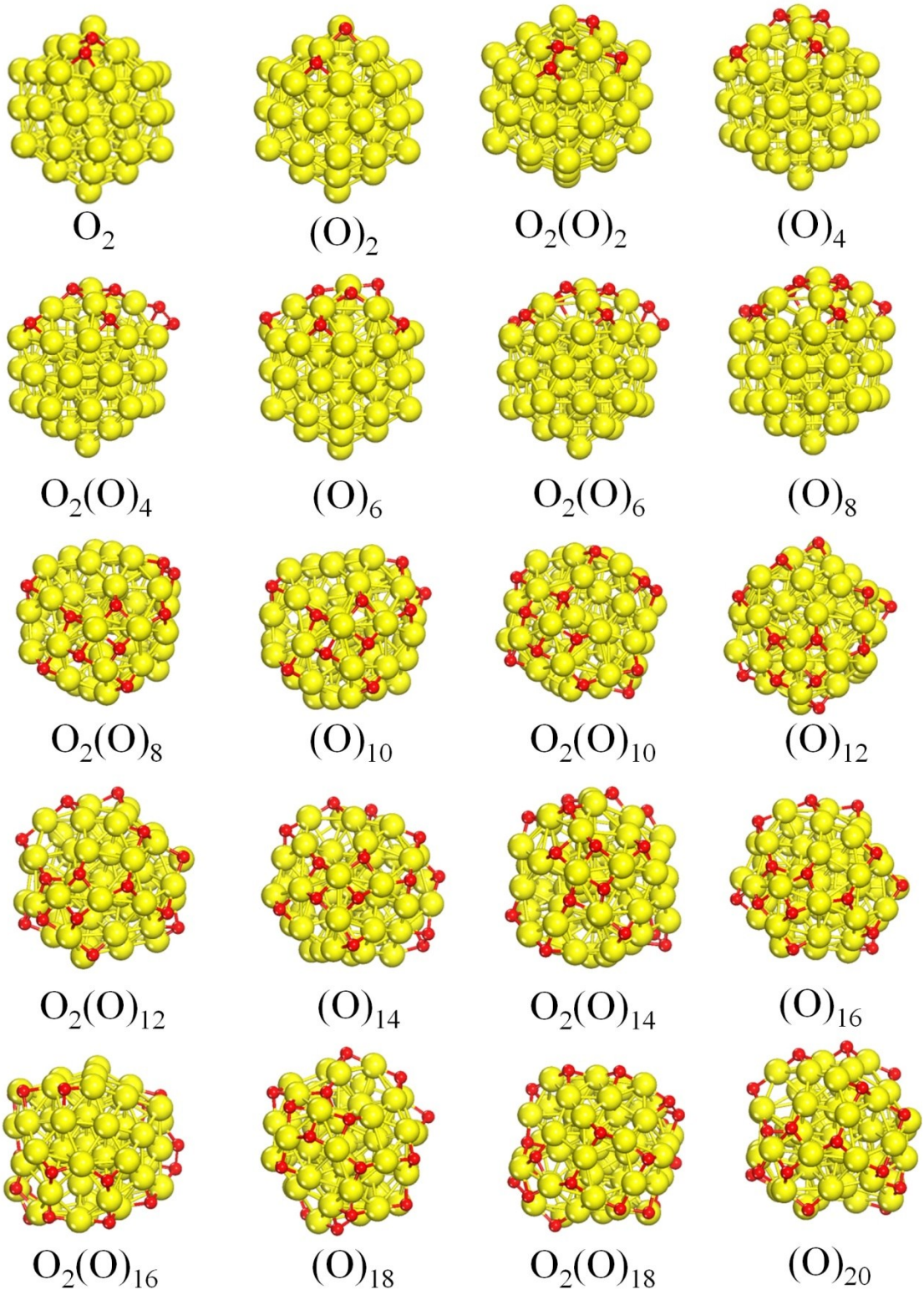
O_2
$(O)_2$
$O_2(O)_2$
$(O)_4$
$O_2(O)_4$
$(O)_6$
$O_2(O)_6$
$(O)_8$
$O_2(O)_8$
$(O)_{10}$
$O_2(O)_{10}$
$(O)_{12}$
$O_2(O)_{12}$
$(O)_{14}$
$O_2(O)_{14}$
$(O)_{16}$
$O_2(O)_{16}$
$(O)_{18}$
$O_2(O)_{18}$
$(O)_{20}$

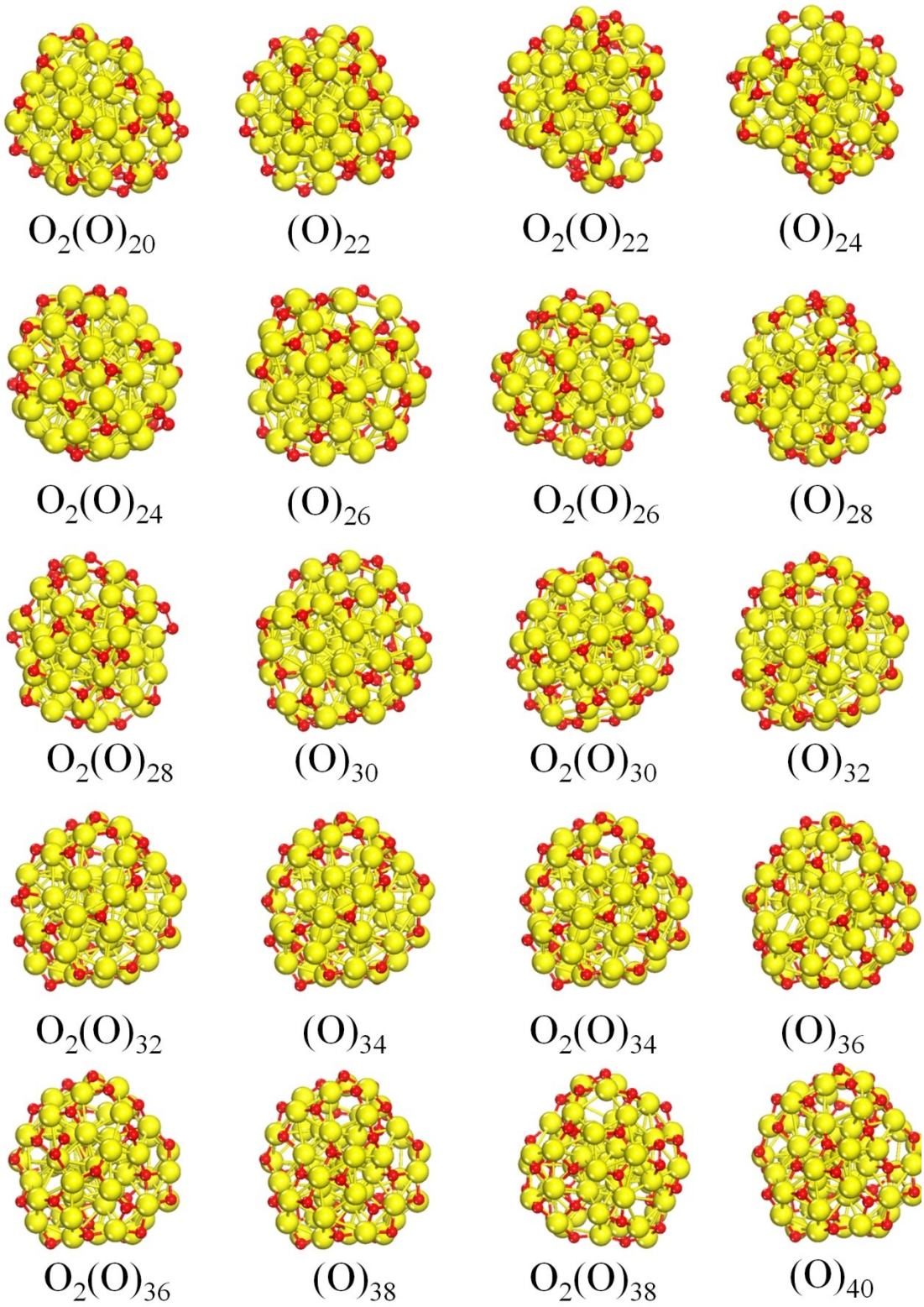

Fig. S6 The full set of geometries for stepwise adsorption and dissociation of O_2 molecules (N = 1-20) on Cu_{55} (Approach 2).

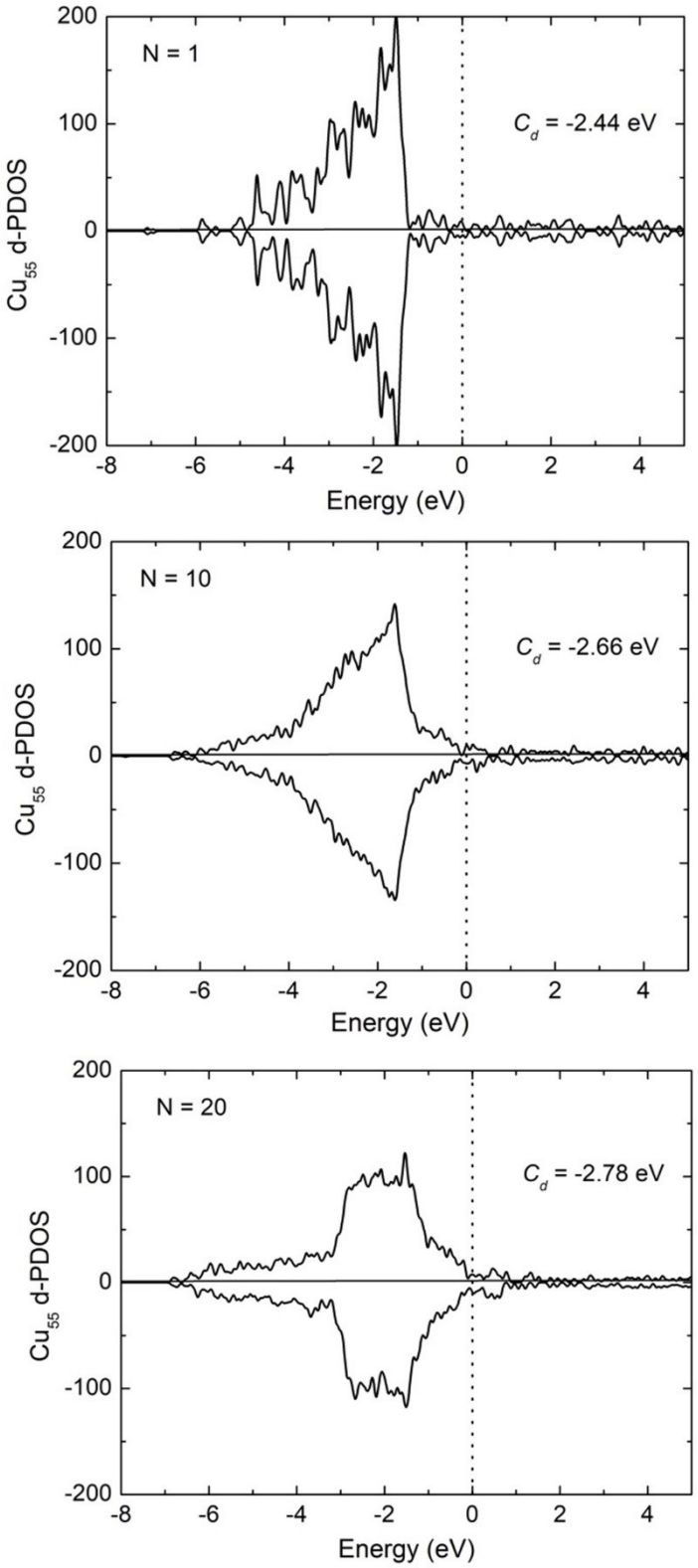

Fig. S7 Spin-polarized Cu_{55} d-projected density of states (d-PDOS) with $(O)_{2N}$ (N = 1, 10, and 20) coverage. The dotted line represents Fermi level at 0.

Table S2 Properties of the stepwise O_2 adsorption and dissociation complexes $Cu_{55}O_{2N}$ (N=1-20, Approach 2).

N ($Cu_{55}O_{2N}$)	$(O_2)_M(O)_{2D}$	$E_a(N)$ (eV)	$< E_a(N) >$ (eV)	Q_{Cu55} (e)	Q_O (e) $(O_2)_M$	$(O)_{2D}$	<Cu-Cu> (Å)
1	O_2	1.29	1.29	1.22	-0.61		2.547
	$(O)_2$	3.41	3.41	1.93		-0.96	2.550
2	$O_2(O)_2$	1.01	2.21	2.99	-0.53	-0.96	2.548
	$(O)_4$	2.66	3.03	4.01		-1.00	2.553
3	$O_2(O)_4$	0.86	2.31	5.15	-0.53	-1.02	2.557
	$(O)_6$	2.94	3.00	5.70		-0.95	2.561
4	$O_2(O)_6$	1.16	2.56	6.87	-0.57	-0.95	2.566
	$(O)_8$	3.31	3.08	8.24		-1.03	2.567
5	$O_2(O)_8$	0.81	2.63	8.97	-0.64	-0.96	2.569
	$(O)_{10}$	3.19	3.10	9.29		-0.92	2.574
6	$O_2(O)_{10}$	1.37	2.81	10.95	-0.63	-0.96	2.574
	$(O)_{12}$	3.60	3.19	11.74		-0.97	2.581
7	$O_2(O)_{12}$	0.98	2.87	12.32	-0.57	-0.93	2.582
	$(O)_{14}$	3.06	3.17	13.34		-0.95	2.597
8	$O_2(O)_{14}$	1.20	2.92	14.27	-0.58	-0.93	2.603
	$(O)_{16}$	2.95	3.14	15.38		-0.96	2.609
9	$O_2(O)_{16}$	1.27	2.93	16.69	-0.51	-0.97	2.611
	$(O)_{18}$	2.57	3.08	17.12		-0.95	2.613
10	$O_2(O)_{18}$	1.08	2.88	18.20	-0.50	-0.95	2.615
	$(O)_{20}$	3.04	3.07	18.66		-0.93	2.618
11	$O_2(O)_{20}$	0.77	2.86	20.88	-0.47	-0.99	2.623
	$(O)_{22}$	2.81	3.05	21.84		-0.99	2.628
12	$O_2(O)_{22}$	0.69	2.80	22.09	-0.37	-0.96	2.627
	$(O)_{24}$	2.63	3.01	23.22		-0.96	2.632
13	$O_2(O)_{24}$	1.41	2.89	24.94	-0.51	-0.99	2.638
	$(O)_{26}$	2.88	3.00	25.00		-0.96	2.639
14	$O_2(O)_{26}$	0.71	2.84	26.57	-0.48	-0.98	2.637
	$(O)_{28}$	2.68	2.98	26.63		-0.95	2.648
15	$O_2(O)_{28}$	0.88	2.84	27.56	-0.49	-0.94	2.652
	$(O)_{30}$	3.12	2.99	27.91		-0.93	2.655
16	$O_2(O)_{30}$	1.01	2.87	29.22	-0.49	-0.94	2.675
	$(O)_{32}$	2.79	2.98	30.15		-0.94	2.677
17	$O_2(O)_{32}$	0.66	2.84	31.16	-0.36	-0.95	2.683
	$(O)_{34}$	1.67	2.90	32.34		-0.95	2.684
18	$O_2(O)_{34}$	0.68	2.74	32.77	-0.34	-0.94	2.689
	$(O)_{36}$	1.69	2.88	33.50		-0.93	2.696
19	$O_2(O)_{36}$	0.39	2.75	33.18	-0.21	-0.91	2.692
	$(O)_{38}$	1.61	2.82	34.76		-0.91	2.697
20	$O_2(O)_{38}$	0.54	2.70	36.09	-0.34	-0.88	2.705
	$(O)_{40}$	1.65	2.77	37.39		-0.93	2.707

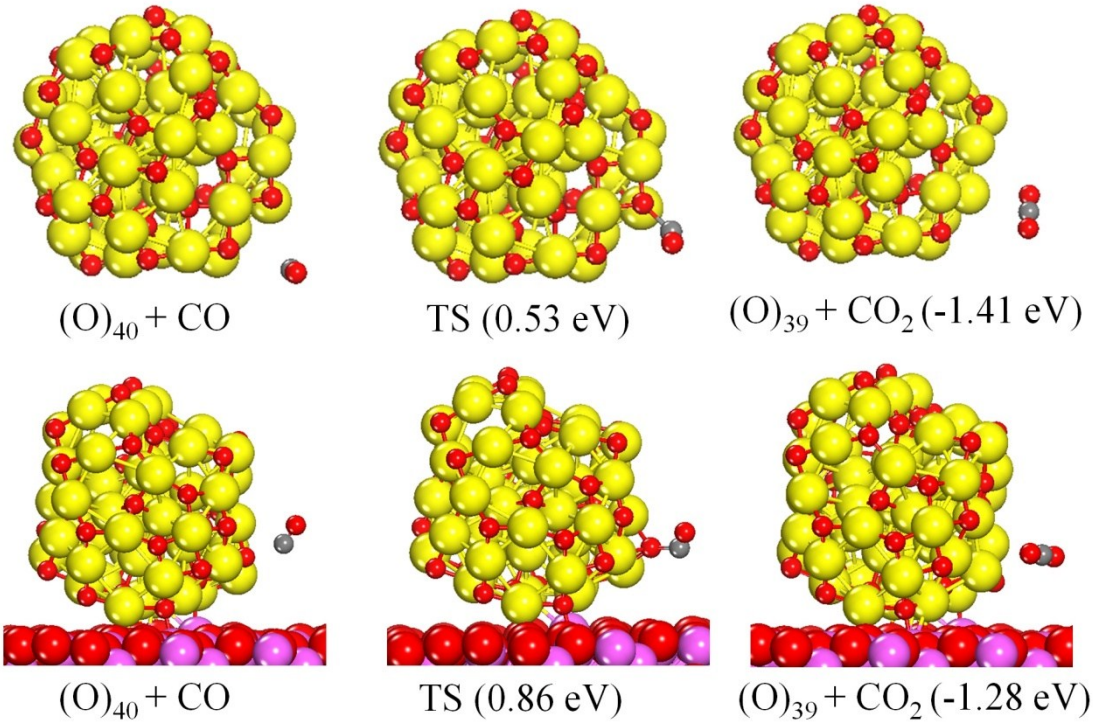

Fig. S8 Structures of the initial state (IS), transition state (TS), and final state (FS) for the catalytic CO oxidation on $Cu_{55}(O)_{40}$ and $Cu_{55}(O)_{40}/\gamma$-$Al_2O_3(100)$ by the Eley−Rideal (ER) mechanism and the energy changes with respect to the IS.